Quantum metrology with superposition spin coherent states: Insights from Fisher information

Yusef Maleki,[1] Marlan O. Scully,[1] and Aleksei M. Zheltikov[1,2,3,4]

[1]*Institute of Quantum Science and Engineering, Department of Physics and Astronomy, College Station, Texas 77843-4242, USA*
[2]*Physics Department, M. V. Lomonosov Moscow State University, Moscow 119992, Russia*
[3]*International Center for Quantum Technologies (Russian Quantum Center), Skolkovo, Moscow Region 143025, Russia*
[4]*Kazan Quantum Center, A. N. Tupolev Kazan National Research Technical University, 420126 Kazan, Russia*

(Received 21 November 2020; accepted 24 August 2021; published 18 November 2021)

We present a closed-form analytical description for the metrological performance of a generic superposition of spin coherent states (SSCS) used as probes for quantum phase estimation. Working in this framework, we derive transparent analytical expressions for the pertinent quantum Fisher information and identify a general class of spin coherent states enabling quantum metrology with Heisenberg-limit precision. Bloch-sphere analysis of antipodal SSCS shows that the phase-estimation precision attainable with such states increases with the distance from the equator of the Bloch sphere, growing from the shot-noise limit level for the equatorial states all the way up to the Heisenberg limit for SSCS that can be represented as superpositions of the poles of the Bloch sphere.

DOI: 10.1103/PhysRevA.104.053712

I. INTRODUCTION

Measurement plays a central role in science, serving as a process whereby scientific hypotheses are scrutinized, theories are tested, and, eventually, new knowledge is gained. In classical physics, better, i.e., more accurate measurements require a larger number of probes N, as the error of measurements is bounded from below by the shot-noise limit (SNL), which scales as $1/\sqrt{N}$. While classical physics views the SNL as the fundamental limit of measurement precision, the quantum theory of measurements relegates it to a more technical status, viz., the limit of precision for measurements performed with N independent probes. Moreover, as one of its central results, quantum theory of measurements predicts [1,2] that the true fundamental limit of measurement precision—the Heisenberg limit (HL)—should instead scale, for suitably correlated probes, as $1/N$. This result paves the ways for ultrahigh-precision spectroscopy, detection of gravitational waves, high-sensitivity magnetometry, microscopy on the nanoscale, and metrology of fundamental physical constants [3–9].

While the HL sets the lower bound on the error of physical measurements, the precision attainable for each specific experimental setting depends on the properties of quantum probes used in this setting. Standing out as an important class of quantum probes enabling measurements with an HL precision are the cat states of the form $\frac{1}{\sqrt{2}}(|N\rangle_a \otimes |0\rangle_b + |0\rangle_a \otimes |N\rangle_b)$, known as NOON states [2,10,11]. Generation of NOON states is conceptually and technically challenging. Several efficient schemes have been proposed within the past few years to confront these challenges via finely tailored quantum-state engineering [12–20]. Yet, the search is ongoing for practical parameter-estimation solutions within a broader class of superposition coherent states that would foster experimental studies and that would help address the issues related to decoherence, dissipation, as well as the high cost and low efficiency of quantum-state generation. As one promising solution, Schrödinger-cat states [21], i.e., superpositions of coherent states $|\pm\alpha\rangle$ have been shown to enable entanglement-enhanced super-resolving phase measurements [22,23] while sustaining a reasonably high immunity to decoherence [24–27]. Quantum states of this class can be generated via laser-assisted entanglement of coherent harmonic-oscillator states of laser-cooled trapped ions [21,28,29], by photon subtraction from a squeezed vacuum state of light [30–32], through optical Fock-state engineering [33,34], as well as by using superconducting qubits [35], cavity QED [36], and linear-optical arrangements [37]. Spin cat states with moderate entanglement have been shown [26] to be more robust against loss than maximally entangled states, enabling high-precision measurements below the SNL level in a dissipative environment. Multiqubit Schrödinger-cat hyper-entanglement [22,38–40] and iterative Schrödinger-cat enlargement [41] have been demonstrated as significant milestones on the way toward practical schemes for quantum information processing, computation, cryptography, and metrology.

Here we examine the performance of a generic superposition of spin coherent states (SSCS) in quantum metrology and identify conditions for attaining the HL precision with such states. We will derive closed-form analytical expressions for the pertinent quantum Fisher information and the related quantum Cramér–Rao bound (CRB) on the error of phase estimation using SSCS. Based on this analysis, we will identify a general class of SSCS enabling quantum metrology with Heisenberg-limit precision. We show that antipodal SSCS that can be represented as superpositions of equatorial states on the pertinent Bloch sphere can only perform at the SNL level of phase-estimation precision. Off the equatorial line, however, the precision of SSCS increases, reaching the HL for the states

that can be represented as superpositions of the poles on the Bloch sphere.

II. SPIN COHERENT STATES FOR PHASE ESTIMATION

We start with a brief review of the main properties of SU(2) spin coherent states. To this end, we consider a spin algebra generated by lowering and raising operators J_- and J_+ and the z-component of the spin J_z such that $[J_+, J_-] = 2J_z$, $[J_z, J_\pm] = \pm J_\pm$. Acting on the ground state of the Dicke basis $|j, -j\rangle$ defined by these operators [42], the rotation operator,

$$R(\theta, \varphi) = \exp\left\{\frac{-\theta}{2}(J_+ e^{-i\varphi} - J_- e^{i\varphi})\right\}, \tag{1}$$

yields a spin coherent state [42],

$$\begin{aligned}|\theta, \varphi, j\rangle &= \exp\left[\frac{\theta}{2}(J_+ e^{-i\varphi} - J_- e^{i\varphi})\right]|j, -j\rangle \\ &= \frac{1}{(1+|\gamma|^2)^j}\sum_{m=-j}^{j}\binom{2j}{j+m}^{\frac{1}{2}}\gamma^{j+m}|j, m\rangle,\end{aligned} \tag{2}$$

where $\gamma = e^{-i\varphi}\tan(\frac{\theta}{2})$.

The inner-product overlap of two spin coherent states is [43]

$$\langle\theta_1, \varphi_1, j|\theta_2, \varphi_2, j\rangle = \frac{(1+\bar{\delta}\gamma)^{2j}}{(1+|\delta|^2)^j(1+|\gamma|^2)^j}, \tag{3}$$

where $\gamma = e^{-i\varphi_1}\tan(\frac{\theta_1}{2})$, $\delta = e^{-i\varphi_2}\tan(\frac{\theta_2}{2})$, and $\bar{\delta}$ is the complex conjugate of δ.

The spin algebra representation defining the coherent state connects to a representation in a two-mode bosonic harmonic-oscillator basis via

$$J_+ = a^\dagger b, \quad J_- = b^\dagger a, \quad J_z = \tfrac{1}{2}(a^\dagger a - b^\dagger b), \tag{4}$$

where a and b are the bosonic annihilation operators of the first and second modes of a harmonic oscillator, which will be referred to hereinafter as the photon annihilation operators.

With N_a and N_b photons in modes a and b, such that $j = \frac{N}{2}$ and $m = \frac{N_a - N_b}{2}$, $N = N_a + N_b$, we find $|N_a\rangle|N_b\rangle \equiv |j, m\rangle$. When all the photons are in one of the two modes, a standard algebra of $J_\pm|j, m\rangle = \sqrt{(j \pm m)(j \pm m + 1)}|j, m \pm 1\rangle$ and $J_z|j, m\rangle = m|j, m\rangle$ yields one of the two states: $|0\rangle \otimes |N\rangle \equiv |j, -j\rangle$ or $|N\rangle \otimes |0\rangle \equiv |j, j\rangle$. A superposition of these two states is a NOON state, $|\mathrm{N00N}\rangle = \frac{1}{\sqrt{2}}(|N, 0\rangle + |0, N\rangle)$, which can now be readily transformed to the Dicke basis as [24]

$$|\mathrm{N00N}\rangle = \frac{1}{\sqrt{2}}(|j, j\rangle + |j, -j\rangle). \tag{5}$$

A NOON state can thus be viewed as a superposition of the two poles of the Bloch sphere. As an outstanding experimental achievement, electron spins in dysprosium atoms have been shown to enable a superposition of opposite-pole spin states with a mesoscopic spin $J = 8$ [44], corresponding to a NOON state with $N = 16$. Such a state has been shown to enhance the sensitivity of magnetic field measurements by a factor 13.9 [44].

As an important finding of earlier studies [25,26], providing a benchmark for our analysis here, a superposition of coherent states of the form

$$|\varphi, j\rangle = \mathcal{N}(|\theta, 0, j\rangle + |\pi - \theta, 0, j\rangle), \tag{6}$$

with $\mathcal{N}$ being the normalization factor, has been shown to surpass the SNL. Given the profoundness of this result for the quantum theory of measurements and its practical significance for quantum metrology, an important question to be asked is whether there are other operationally useful states that can enable measurements with a precision below the SNL. As we will show below in this paper, not only do such states indeed exist but they can also provide a higher precision. In what follows, we will identify such states, derive a closed-form analytical solution for the lower-bound precision that such state can provide in quantum measurements, and specify conditions when this precision reaches the HL.

III. QUANTUM METROLOGY WITH SUPERPOSITION SPIN COHERENT STATES

A. Quantum Fisher information for superposition spin coherent states

In the search for a suitable general class of SSCS capable of performing estimates with a precision below the SNL, we examine superposition states of the form

$$|\psi, j\rangle = \mathcal{N}(|\theta_1, \varphi_1, j\rangle + |\theta_2, \varphi_2, j\rangle), \tag{7}$$

where

$$\mathcal{N} = \left[2 + \frac{(1+\bar{\delta}\gamma)^{2j} + (1+\bar{\gamma}\delta)^{2j}}{(1+|\delta|^2)^j(1+|\gamma|^2)^j}\right]^{-1/2}, \tag{8}$$

where $\bar{\gamma}$ is the complex conjugate of γ.

For a quantitative analysis of the performance of such states in quantum metrology, we consider a generic setting for an estimation of a parameter ξ that shows up in the phase shift $e^{i\xi J_z}$. The error of ξ estimation, $\Delta\xi$ is bounded from below by the quantum CRB [2,8],

$$\Delta\xi_{\mathrm{CRB}} = 1/\sqrt{\mathcal{F}_Q(\rho(\xi))}, \tag{9}$$

where $\mathcal{F}_Q(\rho(\xi)) = Tr[\rho(\xi)L_\xi^2]$ is the quantum Fisher information [2,8], and L_ξ is the symmetric logarithmic derivative, defined by the equation $\partial_\xi\rho(\xi) = (1/2)[\rho(\xi)L_\xi + L_\xi\rho(\xi)]$ for the density matrix $\rho(\xi)$.

Applying the general definition of $\mathcal{F}_Q$ to the SSCS as defined by Eq. (7), we find

$$\mathcal{F}_Q = 4\big(\mathcal{G}_2 + \mathcal{G}_1 - \mathcal{G}_1^2\big), \tag{10}$$

where

$$\mathcal{G}_1 = 2j\mathcal{N}^2\left[\frac{|\gamma|^2}{1+|\gamma|^2} + \frac{|\delta|^2}{1+|\delta|^2} + \mathcal{M}_1\right], \tag{11}$$

$$\mathcal{G}_2 = 2j(2j-1)\mathcal{N}^2\left[\frac{|\gamma|^4}{(1+|\gamma|^2)^2} + \frac{|\delta|^4}{(1+|\delta|^2)^2} + \mathcal{M}_2\right], \tag{12}$$

$$\mathcal{M}_1 = \frac{(1+\bar{\delta}\gamma)^{2j-1}\bar{\delta}\gamma + (1+\bar{\gamma}\delta)^{2j-1}\bar{\gamma}\delta}{(1+|\delta|^2)^j(1+|\gamma|^2)^j},$$

and

$$\mathcal{M}_2 = \frac{(1+\bar{\delta}\gamma)^{2j-2}(\bar{\delta}\gamma)^2 + (1+\bar{\gamma}\delta)^{2j-2}(\bar{\gamma}\delta)^2}{(1+|\delta|^2)^j(1+|\gamma|^2)^j}.$$

Equations (10)– (12) present one of the central results of this study. It is straightforward to see from these equations that $\mathcal{F}_Q$ and, hence the CRB depend only on the phase difference $\phi = \varphi_2 - \varphi_1$ rather than on the individual phases φ_2 and φ_1.

In the case of $j = 1/2$, $\mathcal{F}_Q$ becomes

$$\mathcal{F}_Q = 4\mathcal{N}^2\left[\frac{|\gamma|^2}{1+|\gamma|^2} + \frac{|\delta|^2}{1+|\delta|^2} + \frac{\bar{\delta}\gamma + \bar{\gamma}\delta}{(1+|\delta|^2)^{1/2}(1+|\gamma|^2)^{1/2}}\right]. \tag{13}$$

Since $j = 1/2$ corresponds to $N = 1$, the SNL is equal to the HL, and Eq. (13) does not suggest any quantum enhancement in the precision. Yet, this expression is useful as it provides a closed-form solution that quantifies the metrological performance of spin-1/2 SSCS.

In a special case of $j = 1$, corresponding to two-photon SSCS, $N = 2$, Eqs. (11) and (12) give

$$\mathcal{G}_1 = 2\mathcal{N}^2\left[\frac{|\gamma|^2}{1+|\gamma|^2} + \frac{|\delta|^2}{1+|\delta|^2} + \frac{(1+\bar{\delta}\gamma)\bar{\delta}\gamma + (1+\bar{\gamma}\delta)\bar{\gamma}\delta}{(1+|\delta|^2)(1+|\gamma|^2)}\right], \tag{14}$$

and

$$\mathcal{G}_2 = 2\mathcal{N}^2\left[\frac{|\gamma|^4}{(1+|\gamma|^2)^2} + \frac{|\delta|^4}{(1+|\delta|^2)^2} + \frac{(\bar{\delta}\gamma)^2 + (\bar{\gamma}\delta)^2}{(1+|\delta|^2)(1+|\gamma|^2)}\right], \tag{15}$$

where

$$\mathcal{N} = \left[2 + \frac{(1+\bar{\delta}\gamma)^2 + (1+\bar{\gamma}\delta)^2}{(1+|\delta|^2)(1+|\gamma|^2)}\right]^{-1/2}. \tag{16}$$

Combined with Eq. (10) for $\mathcal{F}_Q$, Eqs. (13) and (14) provide a closed-form solution that quantifies the metrological performance of SSCS with $j = 1$.

B. Phase estimation errors and the HL

For a closer examination of spin-1 states, we consider a superposition of the form

$$|\varphi, j\rangle = \mathcal{N}(|\theta, \varphi, 1\rangle + |\pi - \theta, \varphi + \phi, 1\rangle). \tag{17}$$

For $\phi = \varphi = 0$, this superposition reduces to the superposition state defined by Eq.(6). With $\phi = \pi$, on the other hand, Eq. (17) describes a superposition of two antipodal spin coherent states on the Bloch sphere [27]. As its general property, the CRB $\Delta\xi_{\mathrm{CRB}}$ for the phase estimation error of superposition states (17) is independent of φ. The effect of ϕ is illustrated in Fig. 1, which plots $\Delta\xi_{\mathrm{CRB}}$ as a function of θ. While Eqs. (10), (11), (14), and (15) provide the general solution for the CRB $\Delta\xi_{\mathrm{CRB}}(\theta)$, Fig. 1 illustrates the key properties of the CRB by presenting $\Delta\xi_{\mathrm{CRB}}(\theta)$ for three values of ϕ, viz., $\phi = 0, \pi/2$, and π. One of these ϕ values, $\phi = 0$, allows the solution for $\Delta\xi_{\mathrm{CRB}}(\theta)$ as provided by Eqs. (10), (11), (14), and (15) to be directly benchmarked against the SSCS as defined by Eq. (6). Examination of the case of $\phi = \pi$ will be shown to reveal one of the most remarkable properties of the SSCS as defined by Eq. (17)—the ability to reach the HL for any θ. Finally, $\phi = \pi/2$ is a reasonable intermediate choice for ϕ.

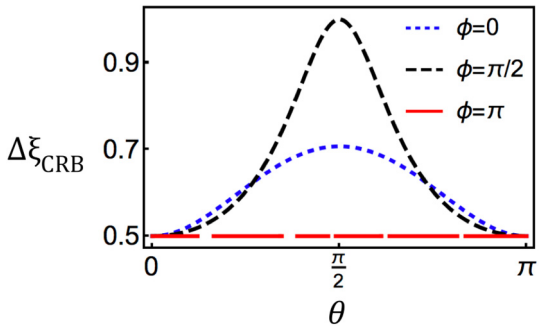

FIG. 1. The CRB $\Delta\xi_{\mathrm{CRB}}$ for the phase estimation error of $j = 1$ SSCS (17) as a function of θ for $\phi = 0$ (dotted blue line), $\phi = \pi/2$ (dashed black line), and $\phi = \pi$ (red line).

As one important finding of this analysis, the antipodal SSCS (17), that is, the SSCS (17) with $\phi = \pi$ (red line in Fig. 1), reach the HL ($\Delta\xi = 1/2$) for any θ. Such SSCS are thus optimal phase estimators. The precision of phase estimation that these states provide is always higher than the precision of the benchmark SSCS as defined by Eq. (6).

As is also seen from Fig. 1, all the SSCS defined by Eq. (17) reach the HL at $\theta = 0$ and π. At these points, the SSCS reduce to a NOON-state superposition of the north and south poles of the Bloch sphere, losing their sensitivity to the azimuthal phase. For $\phi \neq \pi$ SSCS, the phase estimation error reaches its maximum at $\theta = \pi/2$. At this value of θ, both coherent states lie on the $z = 0$ great circle of the Bloch sphere. Finally, SSCS with $\phi = 0$ and $\theta = \pi/2$ perform at the SNL level.

In Fig. 2, we plot the CRB $\Delta\xi_{\mathrm{CRB}}$ for general-form SSCS $|\varphi, j\rangle = \mathcal{N}(|\theta_1, \varphi, 1\rangle + |\theta_2, \varphi + \phi, 1\rangle)$ as a function of θ_1 and θ_2. As is readily seen from these plots, the highest phase-estimation precision for such SSCS is achieved along the $\theta_2 = \pi - \theta_1$ line, which stands out as the darkest line in Figs. 2(a) and 2(b), corresponding to the minimum estimation error, showing, once again, that the antipodal SSCS (17) always reach the HL.

We will now examine the metrological performance of antipodal SSCS with arbitrary j. To this end, we focus on superposition states of the form

$$|\varphi, j\rangle = \mathcal{N}(|\theta, \varphi, j\rangle + |\pi - \theta, \varphi + \phi, j\rangle). \tag{18}$$

As can be seen from Figs. 3(a)–3(c), which present the CRB as a function of θ for various j, the antipodal SSCS

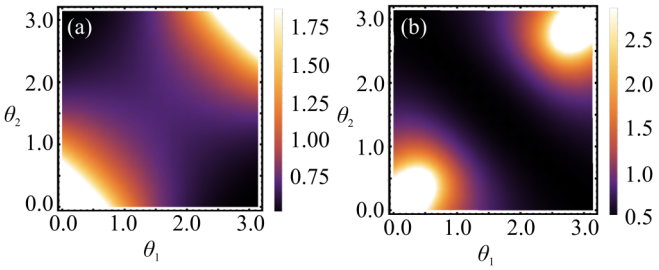

FIG. 2. The CRB $\Delta\xi_{\mathrm{CRB}}$ for the phase estimation error of the $j = 1$ SSCS $|\varphi, j\rangle = \mathcal{N}(|\theta_1, \varphi, 1\rangle + |\theta_2, \varphi + \phi, 1\rangle)$ as a function of θ_1 and θ_2 for $\phi = 0$ (a) and $\phi = \pi$ (b).

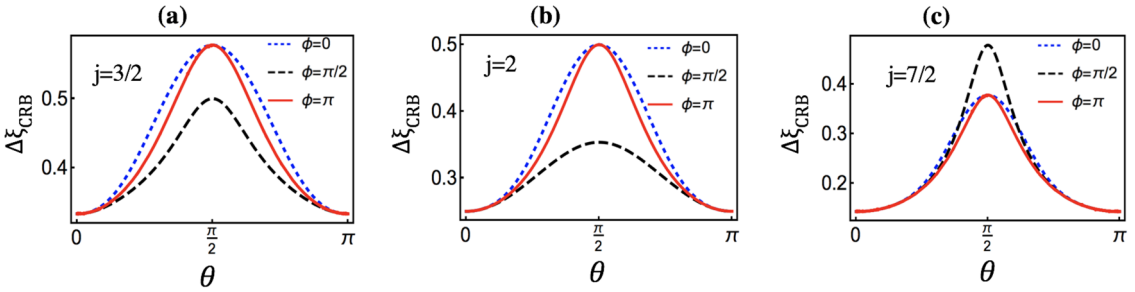

FIG. 3. The CRB as a function of θ for $j = 3/2$ (a), 2(b), and $7/2$ (c) with $\phi = 0$ (dotted blue line), $\phi = \pi/2$ (dashed black line), and $\phi = \pi$ (red line).

as defined by Eq. (18) generally fail to reach the HL. Yet, the precision of phase estimation provided by these states is always higher than the phase-estimation precision provided by SSCS with $\phi = \varphi = 0$, i.e., the superposition state defined by Eq. (6).

C. Bloch-sphere perspective of Heisenberg-limit precision

In a special case of $\bar{\gamma}\delta = -1$, Eq. (10) for antipodal SSCS reduces to

$$\mathcal{F}_Q^A = 4\left[j(2j-1)\frac{1+|\gamma|^4}{(1+|\gamma|^2)^2} + j - j^2\right]. \tag{19}$$

As can be seen from Eq. (19), the HL, $\mathcal{F}_Q^A = N^2 = 4j^2$, can be achieved only when $|\gamma|$ is either zero or infinity, or, equivalently, when θ is either 0 or π. SSCS that satisfy these conditions can be represented as a superposition of the north and south poles of the Bloch sphere, i.e., a NOON state. Another useful insight to be gained from Eq. (19) is that the minimum $\mathcal{F}_Q$ and, hence, maximum CRB is achieved for $|\gamma| = 1$ ($\theta = \pi/2$). The quantum Fisher information in this case is $\mathcal{F}_Q = 2j$. The related maximum of the CRB thus corresponds to the SNL. Geometrically, this means that any antipodal SSCS in the $z = 0$ equatorial circle of the Bloch sphere performs at the SNL precision. Any antipodal SSCS that does not belong to this circle suppresses the SNL, providing quantum enhancement of precision. The phase-estimation precision attainable with antipodal SSCS thus ranges from the SNL, achieved for the states lying on the equator of the Bloch sphere, to the HL, attained with the pole states. The precision increases with the distance from the equator.

D. Fisher-information insights into quantum precision enhancement

It is readily seen from Fig. 3 that, for all the spins examined in these calculations, SSCS with $\phi = \pi$ provide a higher precision compared with SSCS with $\phi = 0$. This property of SSCS can be understood by inspecting their quantum Fisher information for $\phi = 0$ and $\bar{\gamma}\delta = 1$:

$$\mathcal{F}_Q = 4\left[\frac{j(2j-1)}{1+\mathcal{A}^{2j}}\left(1 - \frac{1}{2}\mathcal{A}^2 + \frac{1}{2}\mathcal{A}^{2j}\right) + j - j^2\right], \tag{20}$$

where

$$\mathcal{A} = \frac{2|\gamma|}{1+|\gamma|^2}.$$

At $\theta = \pi/2$, both $\phi = 0$ and $\phi = \pi$ SSCS perform at the SNL level.

As shown by Huang *et al.* [25], for the states (6) with $j \geqslant 20$ and $\theta \leqslant 7\pi/20$, the CRB can be approximated as

$$\Delta\xi_{\mathrm{CRB}} \simeq \left(\frac{1+\tan^2\theta/2}{1-\tan^2\theta/2}\right)N^{-1}, \tag{21}$$

where $N = 2j$.

To gain insights into this relation from the perspective of a more general result as expressed by Eq. (20), we observe that $\mathcal{A}^{2j} \ll 1$ can be met by letting $\theta \neq \pi/2$ and $j \gg 1$, i.e., under conditions that are much more general compared with the inequalities $j \geqslant 20$ and $\theta \leqslant 7\pi/20$ of Ref. [25]. With $\theta \neq \pi/2$ and $j \gg 1$, Eq. (20) leads to

$$\mathcal{F}_Q \simeq 4\left[j^2 - j(2j-1)\frac{1}{2}\mathcal{A}^2\right]. \tag{22}$$

Since $j \gg 1$, $j(2j-1) \simeq 2j^2$, we find

$$\mathcal{F}_Q \simeq 4j^2[1-\mathcal{A}^2] = N^2\left[\frac{1-|\gamma|^2}{1+|\gamma|^2}\right]. \tag{23}$$

Because $|\gamma| = \tan^2\theta/2$, Eq. (23) recovers the result of Huang *et al.* [25]. Moreover, antipodal SSCS with a large spin can also provide $\mathcal{F}_Q$ as defined by Eq. (23).

We now consider SSCS with $\phi = \pi/2$. Closed-form analytical expressions for the quantum Fisher information and the CRB of such states are obtained by combining Eq. (10) with

$$\mathcal{G}_1 = \frac{j}{1+\frac{2^j\cos(\frac{\pi}{2}j)|\gamma|^{2j}}{(1+|\gamma|^2)^{2j}}}\left[1 - \frac{2^{j+1/2}\sin(\frac{\pi}{4}[2j-1])|\gamma|^{2j}}{(1+|\gamma|^2)^{2j}}\right], \tag{24}$$

and

$$\mathcal{G}_2 = \frac{j(2j-1)}{1+\frac{2^j\cos(\frac{\pi}{2}j)|\gamma|^{2j}}{(1+|\gamma|^2)^{2j}}}\left[\frac{1+|\gamma|^4}{(1+|\gamma|^2)^2} - \frac{2^j\sin(\frac{\pi}{2}j)|\gamma|^{2j}}{(1+|\gamma|^2)^{2j}}\right]. \tag{25}$$

In Fig. 3, we compare the behavior of the CRB $\Delta\xi_{\mathrm{CRB}}$ of $\phi = \pi/2$ SSCS as a function of θ with the CRB of $\phi = 0$ and π SSCS. To find the maximum $\Delta\xi_{\mathrm{CRB}}$ values of $\phi = \pi/2$ SSCS [black dashed lines in Figs. 3(a)–3(c)], we set $\theta = \pi/2$ in Eqs. (10), (24), and (25) to derive $\Delta\xi_{\mathrm{CRB}} = 1/2$ for $j = 3/2$, $\Delta\xi_{\mathrm{CRB}} = 1/\sqrt{8}$ for $j = 2$, and $\Delta\xi_{\mathrm{CRB}} \approx 0.48$ for $j = 7/2$. As can be seen from Figs. 3(a) and 3(b), the $\phi = \pi/2$ SSCS with $j = 3/2$ and $j = 2$ provide a higher precision compared with their $\phi = 0$ and π counterparts. For $j = 7/2$,

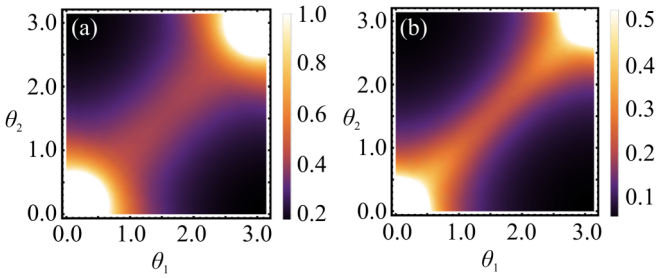

FIG. 4. The CRB $\Delta\xi_{\mathrm{CRB}}$ for $|\varphi, j\rangle = \mathcal{N}(|\theta_1, \varphi, j\rangle + |\theta_2, \varphi + \phi, j\rangle)$ as a function of θ_1 and θ_2 for $\phi = \pi$ with $j = 3$ (a) and $j = 10$ (b).

however, this trend is reversed, as $\phi = 0$ and π states provide a higher precision, especially around $\theta = \pi/2$ [Fig. 3(c)]. We can appreciate now that both the spin and the phase ϕ are significant for the metrological performance of superposition spin coherent states. An important and, perhaps, counterintuitive conclusion to be drawn from Fig. 3 and Eqs. (19)– (23) is that larger photon numbers do not automatically translate into a higher precision. A fine tuning of the phase ϕ is needed for the best metrological performance of high-N SSCS.

In Fig. 4, we present the CRB $\Delta\xi_{\mathrm{CRB}}$ for general-form SSCS $|\varphi, j\rangle = \mathcal{N}(|\theta_1, \varphi, j\rangle + |\theta_2, \varphi + \phi, j\rangle)$ as a function of θ_1 and θ_2 for two values of j: $j = 3$ [Fig. 3(a)] and $j = 10$ [Fig. 3(b)]. For both j, the phase estimation error is seen to be large when $\theta_1 = \theta_2$. The error decreases as the states move apart, toward the opposite poles of the Bloch sphere. The HL precision is achieved when the states reach the respective poles. Thus, the spin coherent states,

$$|\psi, j\rangle = \mathcal{N}(|\theta, \varphi, j\rangle + |\theta, \varphi + \pi, j\rangle), \tag{26}$$

can never surpass the SNL, regardless of their spins and coherence parameters.

For a special case of a single-spin coherent state, $|\psi, j\rangle = |\theta, \varphi, j\rangle$, our general expression for the quantum Fisher information yields

$$\mathcal{F}_Q = 8j\frac{|\gamma|^2}{(1+|\gamma|^2)^2} = 2j\mathcal{A}, \tag{27}$$

showing that a single-spin coherent state never surpasses the SNL.

IV. CONCLUSION

To summarize, we have presented a closed-form analytical description of the metrological performance of a generic SSCS used as probes for quantum phase estimation. Working in this framework, we have derived transparent analytical expressions for the pertinent quantum Fisher information and the related quantum CRB. Based on this analysis, we have identified a general class of superposition spin coherent states enabling quantum metrology with Heisenberg-limit precision. Within this class, the antipodal SSCS $\mathcal{N}(|\theta, \varphi, 1\rangle + |\pi - \theta, \varphi + \phi, 1\rangle)$ have been shown to be of special significance as they reach the HL in phase estimation for any θ. We have demonstrated that both the spin j and the phase ϕ are significant for the metrological performance of general-form superposition spin coherent states $\mathcal{N}(|\theta, \varphi, j\rangle + |\pi - \theta, \varphi + \phi, j\rangle)$. Perhaps counterintuitively, larger photon numbers N do not automatically translate into a higher precision of phase estimation. A fine tuning of ϕ is needed for the best metrological performance of high-N SSCS. Bloch-sphere analysis of antipodal SSCS shows that the phase-estimation precision attainable with such states increases with the distance from the equator of the Bloch sphere, growing from the SNL level for the equatorial states all the way up to the HL for SSCS that can be represented as superpositions of the poles of the Bloch sphere, e.g., NOON states.

ACKNOWLEDGMENTS

This research was supported in part by the Welch Foundation (Grant No. A-1801-20180324), Ministry of Science and Higher Education of the Russian Federation (Project No. 14.Z50.31.0040/17.02.2017), Russian Foundation for Basic Research (Projects No. 18-29-20031, No. 19-02-00473), Russian Science Foundation (Project No. 20-12-00088—ultrabroadband optical science), and the Interdisciplinary Scientific and Educational School of M.V. Lomonosov Moscow State University "Brain, Cognitive Systems, Artificial Intelligence."

[1] V. Giovannetti, S. Lloyd, and L. Maccone, Science **306**, 1330 (2004).
[2] V. Giovannetti, S. Lloyd, and L. Maccone, Nat. Photonics **5**, 222 (2011).
[3] M. Holland and K. Burnett, Phys. Rev. Lett. **71**, 1355 (1993).
[4] J. Bollinger, W. M. Itano, D. Wineland, and D. Heinzen, Phys. Rev. A **54**, R4649 (1996).
[5] S. Pirandola, B. R. Bardhan, T. Gehring, C. Weedbrook, and S. Lloyd, Nat. Photonics **12**, 724 (2018).
[6] B. P. Abbott *et al.*, Phys. Rev. Lett. **116**, 061102 (2016).
[7] T. Ono, R. Okamoto, and S. Takeuchi, Nat. Commun. **4**, 3426 (2013).
[8] P. Cappellaro, J. Emerson, N. Boulant, C. Ramanathan, S. Lloyd, and D. G. Cory, Phys. Rev. Lett. **94**, 020502 (2005).
[9] G. Y. Xiang, B. L. Higgins, D. W. Berry, H. M. Wiseman, and G. J. Pryde, Nat. Photonics **5**, 43 (2011).
[10] A. N. Boto, P. Kok, D. S. Abrams, S. L. Braunstein, C. P. Williams, and J. P. Dowling, Phys. Rev. Lett. **85**, 2733 (2000).
[11] J. P. Dowling, Contemp. Phys. **49**, 125 (2008).
[12] P. Kok, S. L. Braunstein, and J. P. Dowling, J. Opt. B **6**, S811 (2004).
[13] M. F. Riedel, P. Böhi, Y. Li, T. W. Hänsch, A. Sinatra, P. Treutlein, Nature (London) **464**, 1170 (2010).
[14] L. A. Pezze, A. Smerzi, M. K. Oberthaler, R. Schmied, and P. Treutlein, Rev. Mod. Phys. **90**, 035005 (2018).
[15] B. Bell, S. Kannan, A. McMillan, A. S. Clark, W. J. Wadsworth, and J. G. Rarity, Phys. Rev. Lett. **111**, 093603 (2013).
[16] I. Afek, O. Ambar, and Y. Silberberg, Science **328**, 879 (2010).
[17] Y. Maleki and A. M. Zheltikov, Phys. Rev. A **97**, 012312 (2018).
[18] Y. Maleki and A. M. Zheltikov, Sci. Rep. **9**, 16780 (2019).
[19] Q.-P. Su, C.-P. Yang, and S.-B. Zheng, Sci. Rep. **4**, 3898 (2014).

[20] Q.-P. Su, H.-H. Zhu, L. Yu, Y. Zhang, S.-J. Xiong, J.-M. Liu, and C.-P. Yang, Phys. Rev. A **95**, 022339 (2017).
[21] D. J. Wineland, Rev. Mod. Phys. **85**, 1103 (2013).
[22] W.-B. Gao, C.-Y. Lu, X.-C. Yao, P. Xu, O. Guhne, A. Goebel, Y.-A. Chen, C.-Z. Peng, Z.-B. Chen, and J.-W. Pan, Nat. Phys. **6**, 331 (2010)
[23] D. Leibfried, M. D. Barrett, T. Schaetz, J. Britton, J. Chiaverini, W. M. Itano, J. D. Jost, C. Langer, and D. J. Wineland, Science **304**, 1476 (2004).
[24] B. C. Sanders and C. C. Gerry, Phys. Rev. A **90**, 045804 (2014).
[25] J. Huang, M. Zhuang, B. Lu, Y. Ke, and C. Lee, Phys. Rev. A **98**, 012129 (2018).
[26] J. Huang, X. Qin, H. Zhong, Y. Ke, and C. Lee, Sci. Rep. **5**, 17894 (2015).
[27] Y. Maleki and A. M. Zheltikov, J. Opt. Soc. Am. B **37**, 1021 (2020).
[28] C. Monroe, D. M. Meekhof, B. E. King, and D. J. Wineland, Science **272**, 1131 (1996).
[29] M. J. McDonnell, J. P. Home, D. M. Lucas, G. Imreh, B. C. Keitch, D. J. Szwer, N. R. Thomas, S. C. Webster, D. N. Stacey, and A. M. Steane, Phys. Rev. Lett. **98**, 063603 (2007).
[30] A. Ourjoumtsev, R. Tualle-Brouri, J. Laurat, and P. Grangier, Science **312**, 83 (2006).
[31] J. S. Neergaard-Nielsen, B. Melholt Nielsen, C. Hettich, K. Mølmer, and E. S. Polzik, Phys. Rev. Lett. **97**, 083604 (2006).
[32] A. Ourjoumtsev, F. Ferreyrol, R. Tualle-Brouri, and P. Grangier, Nat. Phys. **5**, 189 (2009).
[33] A. E. Ulanov, I. A. Fedorov, D. Sychev, P. Grangier, and A. I. Lvovsky, Nat. Commun. **7**, 11925 (2016).
[34] E. Bimbard, N. Jain, A. MacRae, and A. I. Lvovsky, Nat. Photon. **4**, 243 (2010).
[35] B. Vlastakis, G. Kirchmair, Z. Leghtas, S. E. Nigg, L. Frunzio, S. M. Girvin, M. Mirrahimi, M. H. Devoret, and R. J. Schoelkopf, Science **342**, 607 (2013).
[36] J. M. Raimond, M. Brune, and S. Haroche, Phys. Rev. Lett. **79**, 1964 (1997).
[37] A. Ourjoumtsev, H. Jeong, R. Tualle-Brouri, and P. Grangier, Nature (London) **448**, 1784 (2007).
[38] D. Leibfried, E. Knill, S. Seidelin, J. Britton, R. B. Blakestad, J. Chiaverini, D. B. Hume, W. M. Itano, J. D. Jost, C. Langer, R. Ozeri, R. Reichle, and D. J. Wineland, Nature (London) **438**, 639 (2005).
[39] H. Häffner, W. Hänsel, C. F. Roos, J. Benhelm, D. Chek-al-kar, M. Chwalla, T. Körber, U. D. Rapol, M. Riebe, P. O. Schmidt, C. Becher, O. Gühne, W. Dür, and R. Blatt, Nature **438**, 643 (2005).
[40] C.-Y. Lu, X.-Q. Zhou, O. Gühne, W.-B. Gao, J. Zhang, Z.-S. Yuan, A. Goebel, T. Yang, and J.-W. Panet, Nat. Phys. **3**, 91 (2007).
[41] D. V. Sychev, A. E. Ulanov, A. A. Pushkina, M. W. Richards, I. A. Fedorov, and A. I. Lvovsky, Nat. Phys. **11**, 379 (2017).
[42] G. S. Agarwal, *Quantum Optics* (Cambridge University Press, 2013).
[43] M. Combescure and D. Robert, *Coherent States and Applications in Mathematical Physics* (Springer, Heidelberg, 2012).
[44] T. Chalopin, C. Bouazza, A. Evrard, V. Makhalov, D. Dreon, J. Dalibard, L. A. Sidorenkov, and S. Nascimbene, Nat. Commun. **9**, 1 (2018).